Arabian Journal of Chemistry (2021) **14**, 103312

King Saud University

Arabian Journal of Chemistry

www.ksu.edu.sa
www.sciencedirect.com

ORIGINAL ARTICLE

Effect of advanced oxidation and amino acid addition on antioxidant capability, iron chelating property and anti-cancer activity of tannic acid

Watchareeporn Chariyarangsitham, Saowalak Krungchanuchat, Piyachat Khuemjun, Chalermchai Pilapong *

Center of Excellence for Molecular Imaging (CEMI), Department of Radiologic Technology, Faculty of Associated Medical Sciences, Chiang Mai University, Chiang Mai 50200, Thailand

Received 8 May 2021; accepted 3 July 2021
Available online 14 July 2021

KEYWORDS

Tannic acid;
Oxidized tannic;
Tannic conjugates;
Antioxidant;
Iron chelator;
Anti-cancer

Abstract Although tannic acid (TA) has been shown to exhibit various biological properties, its properties may be hindered by alteration of its chemical structure. To explore the possible alterations in living system-like conditions, we firstly investigated oxidation reaction and amino acid addition of TA in physiological buffered solutions. Evidently, TA was found to be easily oxidized and interacted with amino acids in a phosphate buffered saline solution at 37 °C. The modified TA samples were found to conserve iron-chelating property, but diminish antioxidant capability and anti-cancer activity. As far as biomedical utilizations of TA is concerned, therefore, the structure alterations by above phenomena need to be taken into account. On the other hand, we might also take advantage of advanced oxidation and amino acid addition of TA by pre-treatment of TA according to our described procedures to generate TA derivatives for utilization in specific applications.

1. Introduction

It has been known for long time that polyphenols such as curcuminoids, stilbinenoide, and flavonoids have the potential to prevent and treat many diseases such as cancer, neurodegeneration diseases, etc (Fraga et al., 2019; Spagnuolo et al., 2016; Tresserra-Rimbau et al., 2018). They have been shown to exhibit their bioactivities via various mechanisms such as antioxidation, anti-inflammation, inhibition of peptide aggregation, modulation of autophagy, etc(Andrade et al., 2019; Joseph et al., 2016; Wu et al., 2020). Tannic acid (TA) is a large polyphenol with a molecular mass of 1701.206 g per mole (g / mol) containing gallotannin, trigallic acid, m-digallic, and gallic acid. It is found in vegetables, fruits, and beverages such as tea leaves, guava leaves, grapes, red wine, and bananas. TA exhibits several theraputic potentials via several biological

* Corresponding author.
E-mail address: chalermchai.pilapong@cmu.ac.th (C. Pilapong).
Peer review under responsibility of King Saud University.

ELSEVIER Production and hosting by Elsevier

https://doi.org/10.1016/j.arabjc.2021.103312

properties as antioxidants (Braidy et al., 2017), anti-inflammatories (Luduvico et al., 2020), inhibitors of amyloid peptides aggregation (Soyocak et al., 2019) and anti-cancer (Kim et al., 2019; Nie et al., 2016; Sp et al., 2020). In addition, it has been found that TA has the potential to bind non-transferring bound iron (NTBI), leading to prevention of adverse effects induced by NTBI (Phiwchai et al., 2018; Sahiner, 2021).

According to a toxicology study, TA has low toxicity in rats without mutagenicity and carcinogenicity. It can rapidly be absorbed into the digestive tract to enter the bloodstream and is metabolized to reduce toxicity and for clearance (Nakamura et al., 2003). Compared to the other polyphenols, TA is less studied due to some of its undesirable effects such as causing stomach irritation, inducing protein precipitation, and inhibiting the absorption of iron in the digestive tract. Furthermore, TA is also able to react with biomolecules within the digestive tract, resulting in less absorption (Amarowicz, 2007). When considering the chemical structure of TA, there are a large number of catechol groups that can be oxidized with suitable oxidizing agents (Perkowski et al., 2003) and they interact with other molecules through various reactions. For example, there are thiol-catechol reactions (Brubaker et al., 2010; Lee et al., 2010), amino-catechol reactions (Chen et al., 2018; Qian et al., 2020), boronic acid-catechol reactions (Su et al., 2011), and metal-complex reactions (Guo et al., 2014). As far as the reactions that occur in living system is concerned, oxidization of TA and interaction of catechol groups of TA with free nucleophilic functional groups such as sulfhydryl, amine, amide, indole, and imidazole needs to be taken into account (Bittner, 2006). Such reactions might play a critical role in the biological properties of TA in living system. To the best of our knowledge, the changes in chemical, physical, and biological properties of TA that undergoes oxidation reaction and amino acid addition in physiological-like environment have not been reported clearly. Herein, we aimed to investigate whether TA in physiological buffered solutions with and without amino acids was prone to oxidation and interaction with amino acid, and whether advanced oxidation and amino acid addition of TA affected chemical, physical, and biological properties of TA for example protein precipitation, iron binding capability, radial scavenging activity, and anti-cancer activity.

2. Experiments

2.1. Materials

Ferric chloride hexahydrate ($FeCl_3{\cdot}6H_2O$) was purchased from Fisher Chemicals. Tannic acid ($C_{76}H_{52}O_{46}$) was purchased from Loba Chemie. Roswell Park Memorial Institute (RPMI) 1640, Dulbecco's modified Eagle's medium Ham's F-12 (DMEM/F-12), Penicillin-streptomycin and Trypsin-EDTA were purchased from Caisson Laboratories. Fetal bovine serum (FBS) was purchased from Thermo Fisher Scientific. Collagen type I, ribonuclease A (Rnase A), triton X-100, and propidium iodide (PI) were purchased from US Biological. Dimethyl sulfoxide (DMSO), potassium bromide (KBr), and 7-dichloro- fluorescein diacetate, (H2DCFDA) were purchased from Sigma-Aldrich. L-Lysine, ($C_6H_{14}N_2O_2$), L-Phenylalanine ($C_9H_{11}NO_2$), 3-dimethylthiazol-2,5-diphenyltetrazolium bromide (MTT) were purchased from Bio Basic Inc. Ethyl alcohol and potassium dihydrogen phosphate (KH_2PO_4) were purchased from QRec. Di-Sodium hydrogen phosphate dihydrate (Na_2HPO_4) and tri-sodium citrate were purchased from RCI Labscan Limited. Potassium chloride (KCl), Sodium choride (NaCl), L-cysteine ($C_3H_7NO_2S$), and DMSO d_6 was purchased from Merck. Lymphoprep^{TM} was purchased from Axis-Shield.

2.2. Oxidation and amino acid addition of TA

In order to show that chemical structure of tannic acid can be easily changed in a physiological-like environment, TA was allowed to incubate in PBS pH 7.4 (137 mM NaCl, 2.7 mM KCl, 10 mM Na_2HPO_4, 1.8 mM KH_2PO_4) with and without amino acids such as lysine, phenylalanine, and cysteine. Typically, in order to allow oxidation reaction of TA, TA (0.01 mmol) was incubated in 30 mL of the PBS at 37 °C for different lengths of time. In case of amino acid modified TA, TA (0.01 mmol) was incubated in PBS containnig amino acids (0.03 mmol) at 37 °C for different lengths of time. The obtained solutions were subjected to fllter thru 0.2 μm sterile filter and were further kept at 4 °C for cellular experiments. In addition, the solutions of TA containing amino acids were subjected to purification by Slide-A-Lyzer dialysis Cassettes (2 K MWCO) and were further freeze-dried for further characterizations by FITR and NMR.

2.3. Characterization of different TA samples

UV–vis spectra were determined with Agilent UV–vis spectrophotometer (Agilent 8453, China). The functional groups of different TA samples were investigated by a Fourier transform infrared (FTIR) spectrophotometer (Bruker Tensor 27, Germany) with KBr as the diluting agent over the wavenumber 4000–400 cm^{-1}. Modifications of chemical structure of TA by amino acids were characterized by ^1H NMR spectroscopy (400 MHz, Bruker AVANCE TM, Germany) with DMSO d_6 as the solvent. Mophology of iron-tannic complexes was determined by transmission electron microscope (TEM, JEM-2010, JEOL, Japan).

2.4. Interaction of different TA samples with NTBI in different media

At first, ferric-citrate complexes were prepared in order to use as NTBI model. In typical, 10 mmol of tri-sodium citrate was mixed with 5 mmol of ferric chloride under vigorous stirring. The resulting pale-yellow solution was allowed to equilibrate for 30 min and further subjected to sterilization by using syringe filter (0.2 μm in diameter). To investigate iron binding efficiency of different TA samples, certain amounts of different TA samples (10 μM in final concentration) were mixed with different concentrations of ferric-citrate complexes in different media, including PBS buffer and PBS containing 10% FBS. The UV–Vis absorption spectra were recorded on a UV–vis spectrophotometer (Agilent 8453) at different lengths of incubation time. The iron binding capability of TA samples was obtained by measuring the absorbance of ligand-to-metal charge transfer band at ~525 nm.

2.5. DPPH assay

The antioxidant properties of different TA samples, different amino acids, and ascorbic acid were analyzed by using DPPH assay. In typical experiment, PBS solutions containing different samples (10 μM in final concentration) were mixed with DPPH reagent, and were further incubated for 30 min in the dark. After that, the absorbance of the samples was measured at 520 nm using PBS as blank. The radical scavenging activity was calculated according to the following equation as; $DPPH\ scavenging(\%) = [(A_{control} - A_{sample})/A_{control}] \times 100$, where $A_{control}$ and A_{sample} are the absorbance of blank DPPH solution and sample solution, respectively.

2.6. Protein precipitation assay

In order to examime protein precipitation induced by different TA samples, different concentration of TA samples were incubated with FBS solution for a week (7 days) at 37 °C under 5% CO_2 atmosphere. The protein precipitates were directly observed by naked eye.

2.7. Cell culture

Doxorubicin-resistant human leukemic cells (K562/ADR) were maintained in Roswell Park Memorial Institute (RPMI) 1640 supplemented with 10% FBS and 1% penicillin-streptomycin solution and maintained at 37 °C under 5% CO_2 atmosphere.

Alpha mouse liver 12 (AML-12) cells were cultured in Dulbecco's Modified Eagle Medium: Nutrient Mixture F-12 (DMEM/F-12) supplemented with 10% FBS and 1% penicillin–streptomycin solution and were maintained in a 5% CO_2 atmosphere at 37 °C.

Peripheral blood mononuclear cells (PBMCs) were isolated from healthy human peripheral blood by density gradient centrifugation using Lymphoprep™ according to manufacturer's instructions. The isolated cells were maintained in RPMI 1640 medium with 10% Fetal bovine serum, 1% Penicillin-streptomycin solution and maintained at 37 °C under 5% CO_2 atmosphere. Ethical approval for PBMC experiments was obtained from the AMS Human Research Ethics Committee (AMSEC-61EX-046).

2.8. Cell counting assay

K562/ADR and PBMC cells were seeded in 24-well plates (5×10^4 cells/well) at 37 °C under 5% CO_2 atmosphere overnight. Next, the cells were treated with different TA samples for different lengths of time. At the desired time, the cells were counted by using a flow cytometer (Beckman Coulter's Epics XL-MCL). For the analysis, gated population (only lymphocytes for PBMC) was counted and the cell viability was relatively calculated as the percentage of untreated cells (control)

2.9. MTT assay

AML-12 cells were seeded in 24-well plates (5×10^4 cells/well) and were incubated overnight. Then, the cells were treated with different TA samples for 48 h and 72 h. After treatment, the cells were washed with PBS and incubated with 5 mg/ml of MTT solution for 4 h. Next, the cells were washed with PBS and the intracellular formazan was dissolved in DMSO. The absorbance of the formazan solution was measured with a microplate-reader (Biotek Synergy H4) at 570 nm using DMSO as the blank. The cell viability was relatively calculated as the percentage of untreated cells (control).

2.10. Cell cycle analysis and apoptosis determination

The cells were seeded in 24-well plates ($5x10^4$ cells/well) and were incubated overnight. The cells were treated with different TA samples for different lengths of time (10 μM for TA, TA + Lys and TA + Cys, 20 μM for Taox, and TA + Phe). After the treatment, the cells were harvested and washed twice with PBS solution. Next, the cells were fixed with 70% ethanol for 2 h at 4 °C. The fixed cells were incubated with 5 μL of 10% Triton X, 50 μL of 2 mg/mL RNase A, and 5 μL of 1 mg/mL PI for 20 min at 37 °C. The DNA content of the cells in different cell cycle phases and fractional DNA (apoptosis) was measured with the flow cytometer (PI channel) and the cell cycle distribution was analyzed by using Flowing Software 2.5.0. The percentage of cells in each cell cycle phase was quantified by using markers set within the analysis program.

2.11. Flow cytometry measurment of intracellular ROS (DCFDA staining assay)

The cells were seeded in 24-well plates ($5x10^4$ cells/well) and were incubated overnight. The cells were treated with different TA samples for different lenghts of time (10 μM for TA, TA + Lys and TA + Cys, 20 μM for TAox and TA + Phe). After the treatment, the cells were washed twice with PBS and were then subjected to intracellular ROS measurement by incubating with 0.1 μM H2DCFDA at 37 °C in an incubator for 30 min. Afterward, green fluorescence intensity of DCF (FL1) of the stained cells was measured with the flow cytometer.

2.12. Flow cytometry measurment of lysosome (Acridine orange staining assay)

The cells were seeded in 24-well plates ($5x10^4$ cells/well) and were incubated overnight. The cells were treated with a toxic dose of different TA samples for different lengths of time (10 μM for TA, TA + Lys and TA + Cys, 20 μM for TAox and TA + Phe). After the treatment, the cells were washed twice with PBS and were then subjected to lysosome measurment by incubating with 1.25 μM acridine orange at 37 °C for 10 min. Next, red fluorescence intensity of AO (FL3) of the stained cells was measured with the flow cytometer.

3. Results and discussion

3.1. Oxidation and amino acid addition of TA

It has been reported that catechol in polyphenols can be oxidized to quinone groups in the presence of oxygen (Dai et al., 2019; Xiang et al., 2017). Herein, we attempted to inves-

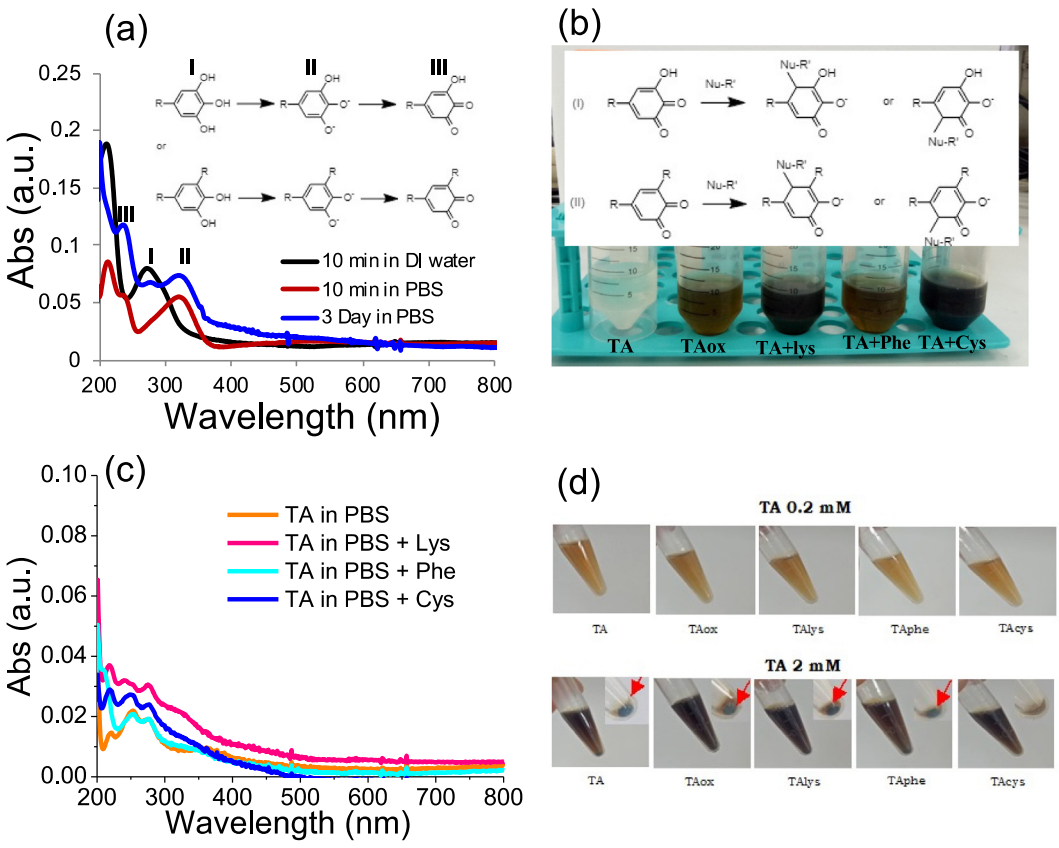

Fig. 1 (a) UV–Vis spectra of TA (1 μM) incubated in DI water and PBS for different lengths of time (inset; possible mechanisms for TA oxidation), (b) photographic image of different TA (0.33 mM) incubated in DI water (TA), PBS (TAox), PBS containing lysine (TA + Lys), PBS containing phenylalanine (TA + Phe), PBS containing cysteine (TA + Cys) (inset; possible mechanisms for amino acid addition reaction of TA), (c) UV–Vis spectra of TA (0.33 mM) incubated in PBS (Taox), PBS containing lysine (TA + Lys), PBS containing phenylalanine (TA + Phe), PBS containing cysteine (TA + Cys), (d) photographic image of different TA samples (0.2 mM and 2 mM) incubated in 10% FBS for a week along with their precipitates (obtained by using 2 mM TA samples).

tigate oxidation reaction of tannic acid dissolved in a simple physiological buffer (PBS buffer, pH7.4). Initially, we measured UV–Vis spectra of TA dissolved in PBS for different lengths of incubation time and compared that to those in DI water. Considering the spectrum of TA in DI water (Fig. 1a), two absorption peaks are clearly observed at 210 nm and 275 nm. Obviously, when we incubated TA in PBS for 10 min, absorption peaks of at 275 nm has a red shift toward 325 nm, which is attributed to deprotonated catechol of TA. As the time passed, significant change in spectra shape of TA in PBS is observed, especially the presence of the absorption peak at 235 nm, which is attributable to oxidized tannic acid. From these results, we can conclude that TA can be oxidized in physiological conditions into semiquinone and o-benzoquinone. Possible oxidation reaction of TA is shown in Fig. 1(inset). It should be noticed that the oxidation yield cannot completely occur in that condition. At least 3 species are present, including (i) protonated TA, (ii) deprotonated TA and (iii) oxidized TA, depending on TA concentration and time of incubation (Rahim et al., 2014). Figure S1 shows UV–Vis spectra of different concentrations of TA dissolved in DI water and PBS for different lengths of incubation time. Clearly, there is no change in spectra shape of TA from dissolving in DI water, indicating no oxidation reaction occurred. However, dramatical change in spectra shape is observed as dissolved in PBS, indicating that oxidation easily occurred in that physiological condition.

It is known that the oxidized catechol can react with various nucleophiles (e.g. -SH, -NH_2) in biomolecules via Michael addition reaction (Liu et al., 2019). Therefore, we aimed to know whether such reaction occurred during autoxidation of TA in PBS. We incubated TA in PBS pH 7.4 containing amino acid (L-lysine, L-cysteine, and L-phenylalanine) at 37 °C for 5 days. It is clearly seen that there are changes in color of solution of TA in PBS (TAox), TA in PBS containing lysine (TA + lys), TA in PBS containing phenylalanine (TA + phe,) and TA in PBS containing cysteine (TA + cys), compared to those in DI water (Fig. 1b). Possible reactions between an oxidized TA and amino acid are shown in Fig. 1b (inset). In order to confirm the existence of amino acid conjugated TA, we purified the conjugated TA samples via a dialysis membrane, and subjected it to further chemical analysis. According to spectroscopic analysis, there is some change in spectra shape of oxidized catechol (230–260 nm) in TA containning amino acid, compared to TA without amino acid, implying that electronic structure of oxidized TA is disturbed by interaction of amino acid (Fig. 1c). In addition, it should be noticed that TAox, TA + lsy, TA + phe, TA + cys seem to have absorption band in visible light region (400–550 nm), which are in accordance with

their deep color. According to FTIR and ^{1}H NMR measurements, all conjugated TA shows the characteristic vibration peaks of amino acid (e.g. N-H stretching, C-N stretching and COO– bending), and several proton signals of amino acid(Gauri et al., 2013) (Figure S2-S6). Above results confirm the formation of TA conjugates in physiology buffer containning amino acid.

3.2. Protein precipitation

It has been reported that TA is capable of inducing protein precipitation via the same mechanism mentioned above. Therefore, we performed protein precipitation assay by incubating different TA samples in fetal bovine serum (FBS) for 7 days. As seen in Fig. 1d, no precipitation is observed when using 0.2 mM in all TA samples, while those of higher concentration (2 mM) are found to induce protein precipitation in FBS, except TA + Cys. This suggests that modification of TA structure with cysteine is capable of reducing nonspecific binding between protein in the serum and TA. This is in agreement with other reports that cysteine is considered to be a zwitterionic amino acid, which is able to reduce nonspecific interaction (Choi et al., 2007). From this result, we might take an advantage of the reduction of protein precipitation by pre-treatment with TA along with cysteine to develop TA conjugates for various applications including nutraceuticals, functional foods, and so on.

3.3. Iron-chelating property

Previously, we demonstrated that TA was able to bind to small iron complexes in physiological media, which can be utilized as a natural iron chelator for chelation therapy (Phiwchai et al., 2018). Herrin, we investigated iron binding capacity of different TA samples in PBS and 10% FBS by measuring absorption peaks of ligand-to-metal charge transfer (LMCT) bands of iron-tannic complexes. Typical UV–Vis spectra exhibits the LMCT peak of iron-tannic complexes at ~500–550 nm, corresponding to a high stable tris-structure of iron-tannic complexes (Fig. 2a,b). The corrected absorbance values are found to increase as the concentration of ferric-citrate complexes increases in both PBS and FBS, demonstrating their capability for iron chelation. By measuring the absorbance of LMCT of different TA samples containing different concentrations of ferric-citrate complexes, we found a good linear correlation between the absorbance and concentration of ferric-citrate complexes over the range of 0–100 μM in all TA samples (Fig. 2a and b), implying that alterations of chemical structure of TA by oxidation and amino acid addition do not strongly affect the ability for iron chelation. This result suggests that all TA samples can be applicable as efficient iron chelators for iron chelation therapy as well as sensors for NTBI detection. Unlike other clinical iron chelators such as deferoxamine, deferiprone and deferasirox, TA samples are able to bind a higher content of iron per molecule and have capability of generating nanosized iron tannic complexes via self-assembly processes (Phiwchai et al., 2018). Fig. 2c shows typical TEM images of nanosized iron-tannic complexes obtained by mixing NTBI with different TA samples. The nanosized complexes provide additional benefits for prevention and treatment such as induction of autophagy and related processes (Phiwchai et al., 2019), as well as the promotion of autophagic cell death (Pilapong et al., 2020).

3.4. Antioxidant capability

Because TA is considered as an anti-antioxidant, we comparatively determined radical scavenging activity of different TA samples, pure amino acids, and ascorbic acid, and reported as a percentage of DPPH scavenging (Lou et al., 2018). The results show that the percentages of DPPH scavenging of TA and TAox are much higher than those observed in other samples for example TA containing amino acids, pure amino acids, and ascorbic acid, indicating a potent antioxidant activity of TA and oxidized TA (Fig. 3a). As is known, assessment of antioxidant activity by DPPH assay rely on capability of the sample to scavenge the DPPH radicals by donating electrons or hydrogen atoms (Formagio et al., 2014). The strongest activity found in oxidized TA is associated with better electron donating capability of the oxidized form of TA. However, TA undergoing amino acid addition reaction is found to decrease antioxidant activity, implying that chemical structure modification of TA by amino acid alters electron donating capability of TA. Surprisingly, however, complex compounds between NTBI and different tannic samples exhibit stronger scavenging activity than TA samples alone (Fig. 3a), which are in good agreement with several tannic nanoplatforms from previous reports (Sahiner et al., 2016; Wei et al., 2020). Stronger scavenging activity found in nanosized iron-tannic complexes may be due to the presence of iron in the tannic complexes that strengthen the electron withdrawing capacity of TA (Yang et al., 2017).

3.5. Anti-cancer activity

Similar to other polyphenols, TA has also been shown to exhibit anti-cancer activity (Kim et al., 2019; Nie et al., 2016; Sp et al., 2020). Herein, we aimed to investigate anti-cancer activity of un-modifed TA and TA that underwent advanced oxidation and amino acid addition. At first, we investigated the effect of different TA samples on cancer cell proliferation. It is seen in Figure S7 that proliferation rate of K562/ADR cells is different in each samples, depending on the concentration. From these results, IC50 values were determined according to dose–response curves, and the results are shown in Table 1. TAox and TA + Phe are found to exhibit lower anti-cancer activity whereas those for TA + Lys and TA + Cys are better, as compared to un-modified TA, depending on time of incubation. This indicates that advanced modifications of chemical structure of TA play a critical role on anticancer activity. It is important to notice that amino acid used in this experiment have no significant effect on cell proliferation. Therefore, it would be solely implied that any change in cell proliferation is caused by modification of chemical structure of TA during their autooxidation and amino acid addition. The results mentioned above demonstrate that alteration of chemical structure of TA strongly affect anticancer activity of TA. However, potential degradation of TA samples mediated by chemicals or enzymes need to be taken into account because it might alter their toxicity in both in vitro and in vivo (Manach et al., 2004; Nakamura et al., 2003). As far as toxicity is concerned, cytotoxicity of different TA samples against normal

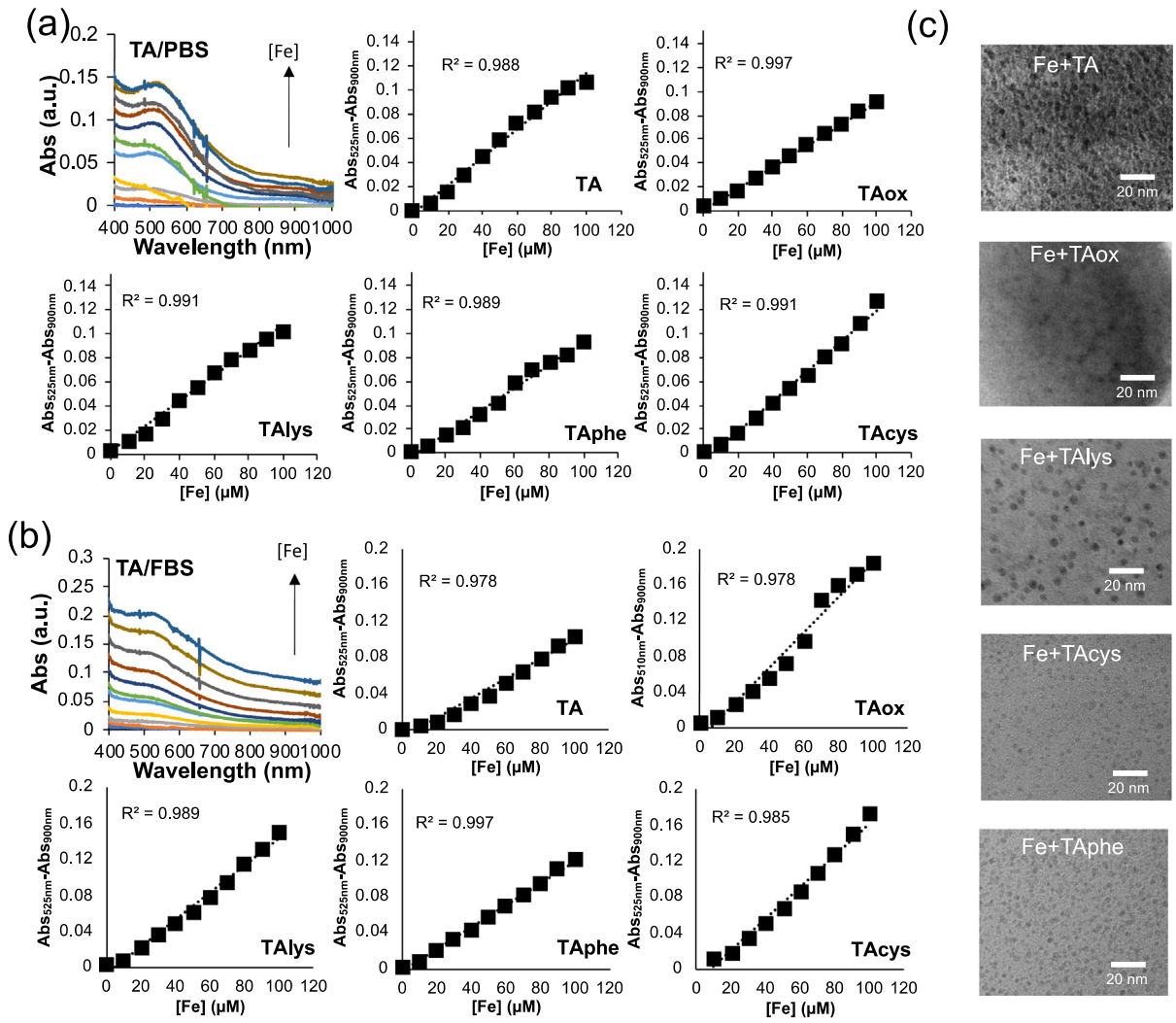

Fig. 2 Typical UV–Vis spectra of TA containing different concentration of ferric citrate complexes, and plots of corrected absorbance (Abs_{525nm}-Abs_{900nm}) versus concentration of ferric citrate complexes measured from different TA samples incubated in (a) PBS and (b) 10 %FBS, (c) typical TEM images of nanosized iron-tannic complexes obtained by mixing iron with different TA samples using 3:1 mol ratios of Fe:TA.

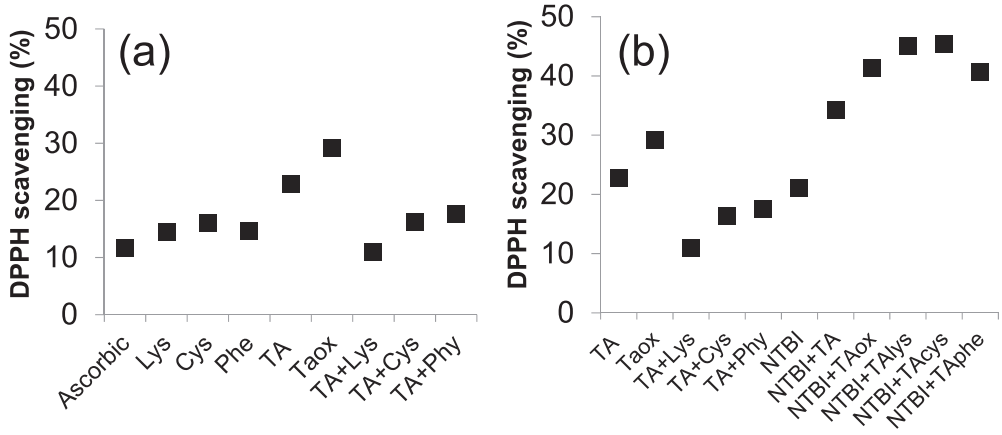

Fig. 3 (a) Percentages of DPPH scavenging activity of ascorbic acid, different amino acids, different TA samples (b) Percentages of DPPH scavenging activity of different TA samples and TA samples containing NTBI.

Table 1 IC50 values obtained from cell counting assay of different TA sample (n = 2).

Samples	IC_{50} (μM)		
	24 h	48 h	72 h
TA	6.2 ± 2.9	8.9 ± 0.1	8.9 ± 0.2
TAox	> 40	22.9 ± 4.7	23.4 ± 3.9
TA + Lys	11.9 ± 6.6	7.1 ± 3.4	6.1 ± 2.7
TA + Phe	18.0 ± 15.8	9.6 ± 2.7	12.2 ± 0.2
TA + Cys	7.8 ± 5.76	6.4 ± 3.6	6.4 ± 0.1

cells was also carried out. In our study, cytotoxicity against normal cells was conducted by using peripheral blood mononuclear cells (PBMCs) and normal hepatocytes (AML-12) as in vitro model. Fig. 4a shows cell viability of K562/ADR cells and PBMCs (lymphocytes population) after treatment with 10 μM of different TA samples for 48 h. It can be seen that TA has significant effect on cell viability of lymphocytes and K562/ADR cells, TAox has no toxic, while amino acid modified TA exhibit less toxic to lymphocytes, as compared to K562/ADR. In addition to PBMCs, hepatocytes are very important for toxicity concerns because TA is metabolized in the liver. AML-12 is a non-transformed mouse hepatocyte cell line that remains as an essential enzyme for TA metabolism. We preliminarily evaluated the effect of different TA samples on cell viability of AML-12 cells using MTT assay. Fig. 4b and 4c show cell viability of AML-12 after incubation with different TA samples for 48 h and 72 h, respectively. The results show that treatment with all TA samples exhibit low hepatotoxicity. Notably, unmodified TA exhibits toxicity in a concentration-dependent manner, but the modified ones were found to be less toxic to the cells, especially for high concentrations of the samples. According to dose–response curve fitting, The IC50 values of unmodified TA were approximately determined as 22.5 and 22.0 μM for 48 h and 72 h of incubation, respectively. For the modified TA samples, the IC50 values of most samples were not able to be determined, indicating that the IC50 values are beyond the tested concentration (> 40 μM). These results suggest that modifications of TA structure by oxidation reaction and amino acid addition are able to prevent liver toxicity mediated by TA. These in vitro findings in toxicity concerns are considered beneficial for predictive information of further in vivo studies or clinical trials.

Although our cell viability analysis provides preliminary results on therapeutic potential of TA samples as an anticancer agent, it neither provides insight into the distribution of the cells in different cell cycle phases nor cell death mechanisms. As far as cell apoptosis and cell cycle disruption are concerned, cell cycle analysis by flow cytometry was carried out. The results demonstrate that TA is capable inducing cell death via apoptosis, in which 80% of cells were found in sub G0 phase (considered as cell apoptosis) at 24 h of induction and up to 90% for those of 48 h and 72 h, indicating a high efficiency for apoptosis induction of unmodified TA (Fig. 5). In cases of modified TA samples, they were found to induce an increasing cell population in the G2/M phase and Sub G0 phase, (but much lower than those observed in un-modified TA) at 24 h. As the time passed, the population of cells in G2/M phase was found to decrease with time, whereas those in Sub G0 phase were found to increase with time, suggesting the sequential events of G2/M arrest followed by apoptosis. In addition, the cell population in SSC/FSC graph (Figure S8) of the treated cells was found to shift to lower FSC (smaller size) and higher SSC (higher internal structure), compared to control. This change is considered as crucial cellular biophysical characteristic of apoptosis cell death. Thus, it can be concluded that the treated cells undergo apoptosis.

It has been reported that a number of polyphenol compounds were capable of inducing cancer cell death via their capability to generate intracellular ROS (D'Angelo et al., 2017; Martino et al., 2019). Herein, we determined the level of ROS after incubation with different TA samples for different lengths of time. As the results show in Fig. 6a, all TA samples are found to increase the level of ROS within the cells after 24 h incubation, compared to untreated cells. Comparatively, unmodified TA seems to have more potent effect on ROS generation, compared to the modified ones. Surprisingly, the high-level ROS was maintained in un-modified TA treated when the incubation time had passed to 72 h, corresponding to apoptosis-inducing potency of TA, but those for modified TA samples were found to decrease (Fig. 6a). This would imply that having a capability to maintain a high level ROS is essential for inducing cell apoptosis by TA. It is important to notice that amino acid used in this experiment have no significant effect on intracellular ROS level (Figure S9). However, induction of cell apoptosis by the modified TA samples might occur through different ways. It is reported that polyphenol

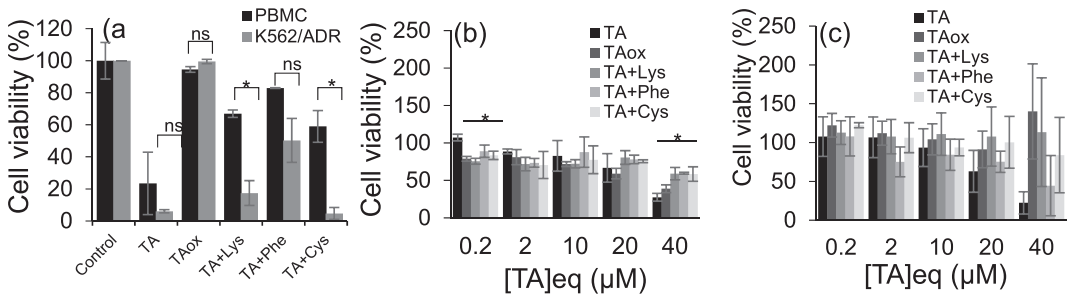

Fig. 4 (a) Cell viability (cell counting) assay of K562/ADR and lymphocytes after treatment with 10 μM of different TA samples for 48 hrs (n = 2), (*$p < 0.05$, ns: not significant by unpaired *t* test). (b,c) Cell viability (MTT) assay of AML-12 cells after treatment with different TA samples for 48 hrs and 72 hrs, respectively (n = 3), (*$p < 0.05$, ns: not significant by one-way ANOVA).

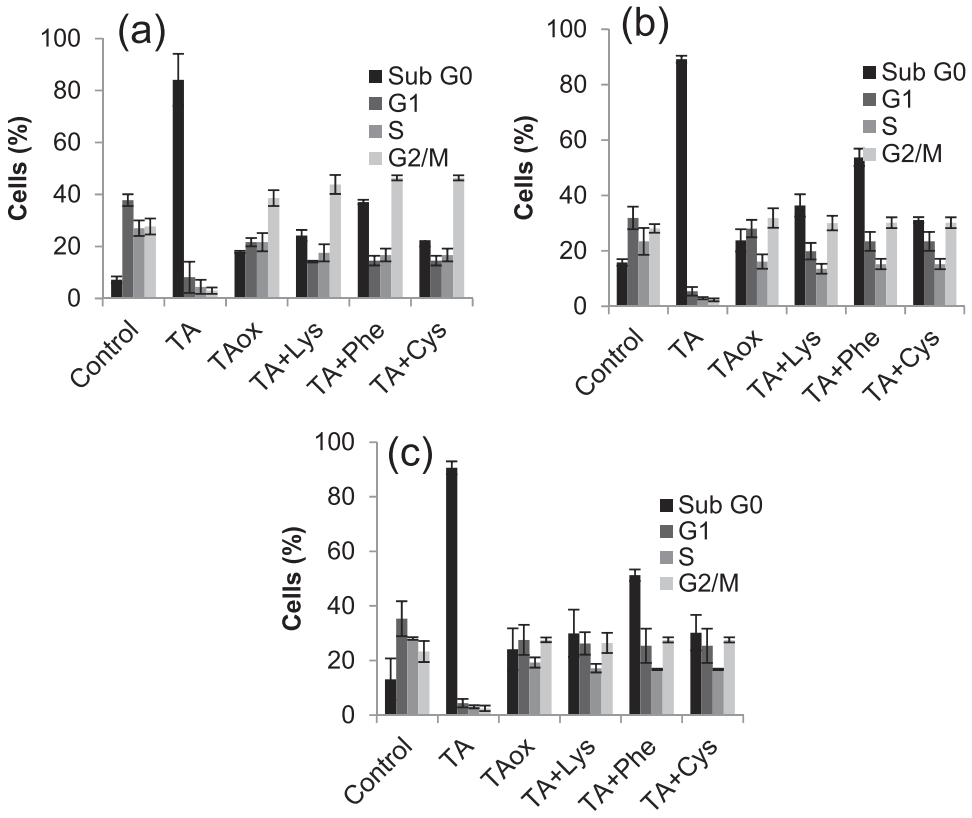

Fig. 5 (a,b,c) Flow cytometric analysis of cell cycle distributions of K562/adr cell after treatment with different TA samples for 24, 48, and 72 hrs, respectively (n = 3). The final concentrations of TA, TA + Lys, TA + Phe and TA + Cys were 10 μM (TA equivalent), while that of TAox was 20 μM.

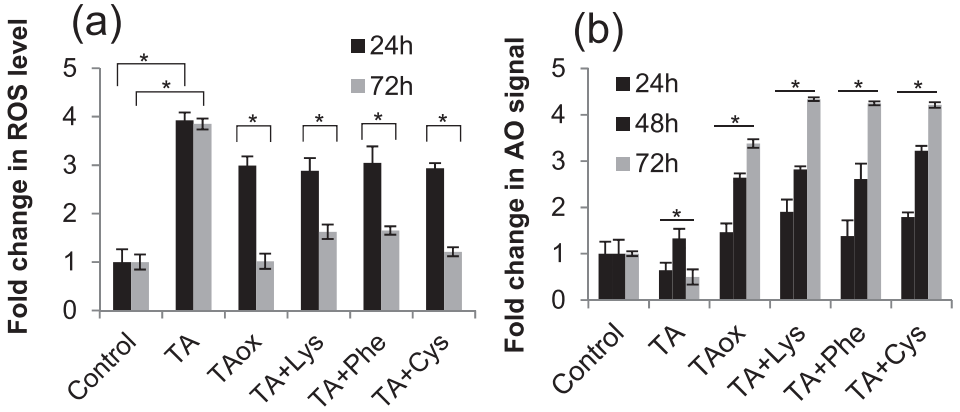

Fig. 6 (a) Flow cytometric analysis of intracellular ROS of K562/ADR cell after treatment with different TA samples for 24 hrs and 72 hrs (n = 3), (*p < 0.05, ns: not significant by unpaired *t* test). (b) Flow cytometric analysis of lysosome of K562/ADR cell after treatment with different TA samples for 24 hrs, 48 hrs, and 72 hrs (n = 3)., (*p < 0.05, ns: not significant by one-way ANOVA). The final concentrations of TA, TA + Lys, TA + Phe and TA + Cys were 10 μM (TA eqivalent), while that of TAox was 20 μM.

can induce autophagic apoptosis (Zhang et al., 2018) and autophagic cell death (Hasima and Ozpolat, 2014). In this context, lysosome has a crucial role in mediating cell death (Kavčič et al., 2017; Kroemer and Jäättelä, 2005). Therefore, we checked lysosome signals by acridine orange staining. For unmodified TA, AO fluorescence signals were found to slightly increase at 48 h of incubation. However, the signal was found to decrease to basal level after longer periods of incubation (72 h), indicating the end of the cellular degradation process (Fig. 6b). This phenomenon is a regular function of lysosomes where they can be activated for cellular degradation and clearance and return to the state of un-activation (basal level.) It should be noticed that low induction of lysosome mediation has no effect on cell apoptosis of TA, as observed from the above results. In contrast, there is a clear enhancement of AO signal (lysosomal signal) in a time-dependent manner in

all modified TA samples. This result suggests that their actions in inducing cell death are totally different than un-modified TA. Possibly, death mechanisms would be mediated through over-activation of lysosomes such as autophagy-mediated apoptosis and autophagy cell death. This corresponds to the results from cell cycle analysis. These findings are of great interest in the context of cancer treatment, especially for apoptosis-resistant cancer cells. However, more studies need to be carried out.

4. Conclusion

TA was prone to undergo oxidation reactions and amino acid addition reactions in physiology buffer, leading to the formation of oxidized TA and of TA - amino acid conjugate derivatives. Surprisingly, iron-chelating property of the modified TA samples was conserved but antioxidant capability and anti-cancer activity were diminished, as compared to un-modified TA. However, advanced oxidation and amino acid addition might provide alternative strategies for improving physico-chemical and biological properties of tannic molecules in order to utilize them in different fields of applications such as nutraceuticals, functional foods, iron chelator, anti-oxidation, and anti-cancer applications.

Declaration of Competing Interest

The authors declare the following financial interests/personal relationships which may be considered as potential competing interests: Patent Application No. 1901007671 (Process for chemical modification of tannic acid) was filed to the Department of Intellectual Property, Thailand.

Acknowledgements

We would like to acknowledge the financial support received from the Center of Excellence on Medical Biotechnology (CEMB), the S&T postgraduate Education and Research Development Office (PERDO), The Commission on Higher Education (CHE), Thailand.

Appendix A. Supplementary material

Supplementary data to this article can be found online at https://doi.org/10.1016/j.arabjc.2021.103312.

References

Amarowicz, R., 2007. Tannins: the new natural antioxidants? Eur. J. Lipid Sci. Technol. 109, 549–551.

Andrade, S., Ramalho, M.J., Loureiro, J.A., Pereira, M.C., 2019. Interaction of natural compounds with biomembrane models: a biophysical approach for the Alzheimer's disease therapy. Colloids Surf. B Biointerfaces 180, 83–92.

Bittner, S., 2006. When quinones meet amino acids: chemical, physical and biological consequences. Amino Acids 30, 205–224.

Braidy, N., Jugder, B.E., Poljak, A., Jayasena, T., Nabavi, S.M., Sachdev, P., Grant, R., 2017. Molecular targets of tannic acid in alzheimer's disease. Curr. Alzheimer Res. 14, 861–869.

Brubaker, C.E., Kissler, H., Wang, L.J., Kaufman, D.B., Messersmith, P.B., 2010. Biological performance of mussel-inspired adhesive in extrahepatic islet transplantation. Biomaterials 31, 420–427.

Chen, S., Xie, Y., Xiao, T., Zhao, W., Li, J., Zhao, C., 2018. Tannic acid-inspiration and post-crosslinking of zwitterionic polymer as a universal approach towards antifouling surface. Chem. Eng. J. 337, 122–132.

Choi, H.S., Liu, W., Misra, P., Tanaka, E., Zimmer, J.P., Itty Ipe, B., Bawendi, M.G., Frangioni, J.V., 2007. Renal clearance of quantum dots. Nat. Biotechnol. 25, 1165–1170.

D'Angelo, S., Martino, E., Ilisso, C.P., Bagarolo, M.L., Porcelli, M., Cacciapuoti, G., 2017. Pro-oxidant and pro-apoptotic activity of polyphenol extract from Annurca apple and its underlying mechanisms in human breast cancer cells. Int. J. Oncol. 51, 939–948.

Dai, Q., Geng, H., Yu, Q., Hao, J., Cui, J., 2019. Polyphenol-based particles for theranostics. Theranostics 9, 3170–3190.

Formagio, A.S., Volobuff, C.R., Santiago, M., Cardoso, C.A., Vieira Mdo, C., Valdevina Pereira, Z., 2014. Evaluation of antioxidant activity, total flavonoids, tannins and phenolic compounds in psychotria leaf extracts. Antioxidants (Basel, Switzerland) 3, 745–757.

Fraga, C.G., Croft, K.D., Kennedy, D.O., Tomás-Barberán, F.A., 2019. The effects of polyphenols and other bioactives on human health. Food Funct. 10, 514–528.

Gauri, S.S., Mandal, S.M., Atta, S., Dey, S., Pati, B.R., 2013. Novel route of tannic acid biotransformation and their effect on major biopolymer synthesis in Azotobacter sp. SSB81. J. Appl. Microbiol. 114, 84–95.

Guo, J., Ping, Y., Ejima, H., Alt, K., Meissner, M., Richardson, J.J., Yan, Y., Peter, K., von Elverfeldt, D., Hagemeyer, C.E., Caruso, F., 2014. Engineering multifunctional capsules through the assembly of metal-phenolic networks. Angew. Chem. Int. Ed. 53, 5546–5551.

Hasima, N., Ozpolat, B., 2014. Regulation of autophagy by polyphenolic compounds as a potential therapeutic strategy for cancer. Cell Death Dis. 5, e1509.

Joseph, S.V., Edirisinghe, I., Burton-Freeman, B.M., 2016. Fruit polyphenols: a review of anti-inflammatory effects in humans. Crit. Rev. Food Sci. Nutr. 56, 419–444.

Kavčič, N., Pegan, K., Turk, B., 2017. Lysosomes in programmed cell death pathways: from initiators to amplifiers. Biol. Chem. 398, 289–301.

Kim, D.A., Choi, H.S., Ryu, E.S., Ko, J., Shin, H.S., Lee, J.M., Chung, H., Jun, E., Oh, E.S., Kang, D.H., 2019. Tannic acid attenuates the formation of cancer stem cells by inhibiting NF-κB-mediated phenotype transition of breast cancer cells. Am. J. Cancer Res. 9, 1664–1681.

Kroemer, G., Jäättelä, M., 2005. Lysosomes and autophagy in cell death control. Nat. Rev. Cancer. 5, 886–897.

Lee, Y., Chung, H.J., Yeo, S., Ahn, C.H., Lee, H., Messersmith, P.B., Park, T.G., 2010. Thermo-sensitive, injectable, and tissue adhesive sol-gel transition hyaluronic acid/pluronic composite hydrogels prepared from bio-inspired catechol-thiol reaction. Soft Matter 6, 977–983.

Liu, J., Yong, H., Yao, X., Hu, H., Yun, D., Xiao, L., 2019. Recent advances in phenolic-protein conjugates: Synthesis, characterization, biological activities and potential applications. RSC Adv. 9, 35825–35840.

Lou, W., Chen, Y., Ma, H., Liang, G., Liu, B., 2018. Antioxidant and α-amylase inhibitory activities of tannic acid. J. Food Sci. Technol. 55, 3640–3646.

Luduvico, K.P., Spohr, L., Soares, M.S.P., Teixeira, F.C., de Farias, A.S., Bona, N.P., Pedra, N.S., de Oliveira Campello Felix, A., Spanevello, R.M., Stefanello, F.M., 2020. Antidepressant Effect and Modulation of the Redox System Mediated by Tannic Acid on Lipopolysaccharide-Induced Depressive and Inflammatory Changes in Mice. Neurochem. Res. 45, 2032-2043.

Manach, C., Scalbert, A., Morand, C., Rémésy, C., Jiménez, L., 2004. Polyphenols: food sources and bioavailability. Am. J. Clin. Nutr. 79, 727–747.

Martino, E., Vuoso, D.C., D'Angelo, S., Mele, L., D'Onofrio, N., Porcelli, M., Cacciapuoti, G., 2019. Annurca apple polyphenol extract selectively kills MDA-MB-231 cells through ROS generation, sustained JNK activation and cell growth and survival inhibition. Sci. Rep. 9, 13045.

Nakamura, Y., Tsuji, S., Tonogai, Y., 2003. Method for analysis of tannic acid and its metabolites in biological samples: application to tannic acid metabolism in the rat. J. Agric. Food Chem. 51, 331–339.

Nie, F., Liang, Y., Jiang, B., Li, X., Xun, H., He, W., Lau, H.T., Ma, X., 2016. Apoptotic effect of tannic acid on fatty acid synthase over-expressed human breast cancer cells. Tumour biol. 37, 2137–2143.

Perkowski, J., Dawidow, U., Jóźwiak, W.K., 2003. Advanced oxidation of tannic acid in aqueous solution. Ozone Sci. Eng. 25, 199–209.

Phiwchai, I., Chariyarangsitham, W., Phatruengdet, T., Pilapong, C., 2019. Ferric-tannic nanoparticles increase neuronal cellular clearance. ACS Chem. Neurosci. 10, 4136–4144.

Phiwchai, I., Yuensook, W., Sawaengsiriphon, N., Krungchanuchat, S., Pilapong, C., 2018. Tannic acid (TA): a molecular tool for chelating and imaging labile iron. Eur. J. Pharm. Sci. 114, 64–73.

Pilapong, C., Phatruengdet, T., Krungchanuchat, S., 2020. Autophagic stress; a new cellular response to nanoparticles. Could it be a new strategy for inhibition of liver cancer cell invasion and metastasis? Nanoscale 12, 6556–6561.

Qian, Y., Chen, S., He, C., Ye, C., Zhao, W., Sun, S., Xie, Y., Zhao, C., 2020. Green fabrication of tannic acid-inspired magnetic composite nanoparticles toward cationic dye capture and selective degradation. ACS Omega 5, 6566–6575.

Rahim, M.A., Ejima, H., Cho, K.L., Kempe, K., Müllner, M., Best, J. P., Caruso, F., 2014. Coordination-driven multistep assembly of metal-polyphenol films and capsules. Chem. Mater. 26, 1645–1653.

Sahiner, N., 2021. Self-crosslinked ellipsoidal poly(tannic acid) particles for bio-medical applications. Molecules (Basel, Switzerland) 26, 2429.

Sahiner, N., Sagbas, S., Sahiner, M., Demirci, S., 2016. Degradable tannic acid/polyethyleneimine polyplex particles with highly antioxidant and antimicrobial effects. Polym. Degrad. Stab. 133, 152–161.

Soyocak, A., Kurt, H., Cosan, D.T., Saydam, F., Calis, I.U., Kolac, U.K., Koroglu, Z.O., Degirmenci, I., Mutlu, F.S., Gunes, H.V., 2019. Tannic acid exhibits anti-inflammatory effects on formalin-induced paw edema model of inflammation in rats. Hum. Exp. Toxicol. 38, 1296–1301.

Sp, N., Kang, D.Y., Jo, E.S., Rugamba, A., Kim, W.S., Park, Y.M., Hwang, D.Y., Yoo, J.S., Liu, Q., Jang, K.J., Yang, Y.M., 2020. Tannic acid promotes TRAIL-induced extrinsic apoptosis by regulating mitochondrial ROS in human embryonic carcinoma cells. Cells 9, 282.

Spagnuolo, C., Napolitano, M., Tedesco, I., Moccia, S., Milito, A., Russo, G.L., 2016. Neuroprotective role of natural polyphenols. Curr Top Med Chem. 16, 1943–1950.

Su, J., Chen, F., Cryns, V.L., Messersmith, P.B., 2011. Catechol polymers for pH-responsive, targeted drug delivery to cancer cells. J. Am. Chem. Soc. 133, 11850–11853.

Tresserra-Rimbau, A., Lamuela-Raventos, R.M., Moreno, J.J., 2018. Polyphenols, food and pharma. Current knowledge and directions for future research. Biochem. Pharmacol. 156, 186–195.

Wei, Z., Wang, L., Tang, C., Chen, S., Wang, Z., Wang, Y., Bao, J., Xie, Y., Zhao, W., Su, B., Zhao, C., 2020. Metal-phenolic networks nanoplatform to mimic antioxidant defense system for broad-spectrum radical eliminating and endotoxemia treatment. Adv. Funct. Mater. 30, 2002234.

Wu, M., Luo, Q., Nie, R., Yang, X., Tang, Z., Chen, H., 2020. Potential implications of polyphenols on aging considering oxidative stress, inflammation, autophagy, and gut microbiota. Crit. Rev. Food. Sci. Nutr, 1–19.

Xiang, S., Yang, P., Guo, H., Zhang, S., Zhang, X., Zhu, F., Li, Y., 2017. Green Tea Makes Polyphenol Nanoparticles with Radical-Scavenging Activities. Macromol, Rapid Commun, p. 38.

Yang, Q., Zhao, C., Zhao, J., Ye, Y., 2017. Synthesis and neuroprotective effects of the complex nanoparticles of iron and sapogenin isolated from the defatted seeds of Camellia oleifera. Pharm. Biol. 55, 428–434.

Zhang, Z., Liu, Z., Chen, J., Yi, J., Cheng, J., Dun, W., Wei, H., 2018. Resveratrol induces autophagic apoptosis via the lysosomal cathepsin D pathway in human drug-resistant K562/ADM leukemia cells. Exp. Ther. Med. 15, 3012–3019.